Review

Imaging findings of intrahepatic cholangiocarcinoma for prognosis prediction and treatment decision-making: a narrative review

Running title: Imaging findings for iCCA

Jun Gu Kang[1,2], Taek Chung[3], Dong Kyu Kim[1,2], Hyungjin Rhee[1,2]*

[1]Department of Radiology, Severance Hospital, Yonsei University College of Medicine, Seoul, Korea

[2]Research Institute of Radiological Sciences, Center for Clinical Imaging Data Science, and Institute for Innovation in Digital Healthcare, Yonsei University College of Medicine, Seoul, Korea

[3]Department of Pathology, Severance Hospital, Yonsei University College of Medicine, Seoul, Korea

*Corresponding author: Hyungjin Rhee, Department of Radiology, Severance Hospital, Yonsei University College of Medicine, 50-1 Yonsei-ro, Seodaemun-gu, Seoul 03722, Korea, E-mail: hjinrhee@yuhs.ac

Abstract

Intrahepatic cholangiocarcinoma (iCCA) is a heterogeneous bile duct adenocarcinoma with a rising global incidence and a poor prognosis. This review aims to present a comprehensive overview of the most recent radiological research on iCCA, focusing on its histopathologic subclassification and the use of imaging findings to predict prognosis and inform treatment decisions. Histologically, iCCA is subclassified into small

duct (SD-iCCA) and large duct (LD-iCCA) types. SD-iCCA typically arises in the peripheral small bile ducts and is often associated with chronic hepatitis or cirrhosis. It presents as a mass-forming lesion with a relatively favorable prognosis. LD-iCCA originates near the hepatic hilum, is linked to chronic bile duct diseases, and exhibits more aggressive behavior and poorer outcomes. Imaging is essential for differentiating these subtypes and assessing prognostic factors like tumor size, multiplicity, vascular invasion, lymph node metastasis, enhancement patterns, and intratumoral fibrosis. Imaging-based prognostic models have demonstrated predictive accuracy comparable to traditional pathological staging systems. Furthermore, imaging findings are instrumental in guiding treatment decisions, including those regarding surgical planning, lymphadenectomy, neoadjuvant therapy, and the selection of targeted therapies based on molecular profiling. Advancements in radiological research have improved our understanding of iCCA heterogeneity, facilitating prognosis prediction and treatment personalization. Imaging findings assist in subclassifying iCCA, predicting outcomes, and informing treatment decisions, thus optimizing patient management. Incorporating imaging-based approaches into clinical practice is crucial for advancing personalized medicine in the treatment of iCCA. However, further high-level evidence from international multicenter prospective studies is required to validate these findings and increase their clinical applicability.

Keywords: Intrahepatic cholangiocarcinoma; Diagnostic imaging; Histopathology; Prognosis; Precision medicine

Introduction

Background

Cholangiocarcinoma (CCA) is an adenocarcinoma characterized by differentiation of the bile duct epithelium. Based on its anatomical location, CCA is classified into intrahepatic CCA (iCCA), perihilar CCA (pCCA), and distal CCA (dCCA) [1,2]. CCAs located more peripherally than the second confluence of the bile ducts are classified as iCCA, those situated between the second confluence and the cystic duct insertion site on the common bile duct are categorized as pCCA, and those found distal to the cystic duct insertion are

classified as dCCA [3]. iCCAs account for 10% to 20% of all CCAs, while pCCAs (50% to 60%) and dCCAs (20% to 30%) are more common [3]. However, while the rates of pCCA and dCCA are decreasing, the age-standardized incidence of iCCA has been rising globally over the past few decades, necessitating closer attention [3]. iCCA is the second most common primary liver cancer after hepatocellular carcinoma (HCC) and has a worse prognosis than HCC [4]. Recently, our understanding of iCCA has improved, and it is now recognized as a heterogeneous tumor with diverse etiology, clinical presentation, pathology, and genetic characteristics. The clinical significance of this heterogeneity is being increasingly recognized.

iCCA often presents as a mass with variable shapes, including lobulated or irregular contours, and may be associated with bile duct dilatation, vascular encasement, and regional lymph node metastasis [5]. The enhancement patterns observed on dynamic computed tomography (CT) or magnetic resonance imaging (MRI) are diverse; typically, peripheral enhancement is evident in the arterial phase, followed by centripetal enhancement in later phases [6,7]. On MRI, most iCCAs exhibit high signal intensity on T2-weighted images relative to the surrounding liver parenchyma, display diffusion restriction on diffusion-weighted images, and appear hypointense in the hepatobiliary phase when gadoxetic acid is used as a contrast medium [6-8]. The imaging characteristics of iCCA are heterogeneous, reflecting the recently recognized diversity of the disease. Accumulating evidence suggests that these imaging features can be clinically applied to predict prognosis and guide treatment decisions [9,10].

Objectives

This review provides a comprehensive overview of recent radiological research on iCCA, emphasizing its histopathological subclassification as well as imaging findings that aid in predicting the prognosis of iCCA and in making treatment decisions.

Ethics statement

As this study is based on a review of the literature, neither institutional review board approval nor informed consent was required. However, informed consent was obtained for the six figures included in this review.

Histopathologic subclassification of iCCA

In the fifth edition of the World Health Organization classification, updated in 2019, a new histological subclassification of iCCA was introduced, delineating small duct (SD-iCCA) and large duct (LD-iCCA) types [11,12]. SD-iCCA and LD-iCCA are distinct not only in their histopathological morphology but also in their etiology, tumor location, gross morphology, histopathological characteristics such as invasiveness and vascularity, molecular features, and prognosis **(Table 1).**

SD-iCCA typically arises in the small bile ducts within the peripheral liver, often in the context of chronic hepatitis and cirrhosis. It is characterized by an exclusively mass-forming (MF) gross morphology [13]. Histologically, SD-iCCA consists of cuboidal or low columnar cells arranged in a tubular or cord-like glandular pattern. Compared to LD-iCCA, SD-iCCA is less frequently associated with aggressive pathological features, such as perineural invasion, vascular invasion, and lymph node metastasis [14]. It also tends to have a higher microvascular density (MVD) and exhibits necrosis less frequently. Overall, SD-iCCA has a more favorable prognosis than LD-iCCA [15,16].

LD-iCCA typically originates in the large bile ducts near the hilum and is often associated with underlying chronic bile duct diseases such as hepatolithiasis, liver fluke infestation, or primary sclerosing cholangitis [13]. LD-iCCA frequently arises from a multistep carcinogenesis process, with well-known precursor lesions including biliary intraepithelial neoplasia and intraductal papillary neoplasm of the bile duct [17]. It usually develops from either periductal-infiltrating (PI) or intraductal-growing (IG) tumors of the large bile duct [14]. These tumors can further evolve into the MF type or present as a hybrid of the MF and either the PI or the IG type [18]. Compared to the SD variant, LD-iCCA more frequently exhibits perineural invasion, vascular invasion, and lymph node metastasis; it also displays lower MVD and more frequent necrosis [14,19]. LD-iCCA has a poorer prognosis than SD-iCCA due to its high invasiveness, which leads to frequent recurrence after curative surgical resection and resistance to chemotherapy [20,21].

Utilizing imaging findings to predict prognosis in iCCA

Imaging assessment of the American Joint Committee on Cancer, Eighth Edition, tumor-node-metastasis staging system

The prognosis of iCCA in clinical settings is generally stratified using the eighth edition of the American Joint Committee on Cancer (AJCC) staging system. This system incorporates the tumor, node, metastasis (TNM) classification [22] and was developed and validated through pathological assessment of tumor involvement [22-25]. In iCCA staging, the T category is defined by several factors, including the size of the tumor (with a threshold of 5 cm), the number of tumors present, vascular invasion, visceral peritoneal perforation, and invasion of extrahepatic organs. The N category signifies the presence of regional lymph node metastasis, while the M category indicates distant metastasis. Although TNM staging should be definitively determined through pathological examination of resectable tumors, imaging-based staging is commonly employed to predict prognosis and guide treatment decisions for tumors prior to surgical resection or those deemed unresectable.

The eighth edition of the AJCC provides brief guidance on the clinical TNM classification for iCCA, noting that both contrast-enhanced CT and MRI are valuable for detecting tumors larger than 2 cm and assessing vascular involvement. Additionally, it indicates that magnetic resonance cholangiopancreatography can offer additional insights into the extent of disease. However, recent clinical practice guidelines from the European Association for the Study of the Liver and the International Liver Cancer Association (EASL-ILCA) recommend MRI over CT for the staging of iCCA [2]. This guidance is supported by a multicenter retrospective study that directly compared these modalities and revealed the superiority of MRI in staging MF-iCCAs, especially for tumors classified as T1b, T2, and T3/T4. Specifically, MRI displayed better performance in predicting T category components, such as tumor multiplicity, vascular invasion, and visceral peritoneal invasion [26].

Tumor size and multiplicity: The eighth edition AJCC staging system for iCCA categorizes solitary tumors as T1a or T1b, depending on whether the tumor is larger or smaller than 5 cm. This classification is underpinned by multiple studies demonstrating that tumors exceeding 5 cm are linked to comparatively poor survival outcomes and a high likelihood of recurrence [27-29]. Recent research has confirmed the reliability of

preoperative imaging for accurately estimating iCCA tumor size, revealing a median difference of less than 0.5 cm between pathological and radiological measurements [30]. Furthermore, a study comparing the effectiveness of CT and MRI for determining iCCA tumor size reported no significant difference between these modalities [26].

Tumor multiplicity is another key determinant for the T category in the AJCC staging system, with its presence categorizing a tumor as T2. Multiplicity is defined as the presence of satellitosis, multifocal tumors, or intrahepatic metastasis [22]. Studies have demonstrated that tumor multiplicity is linked to poorer overall survival and a higher risk of tumor recurrence after resection [31,32]. As previously noted, a recent study showed MRI to be superior to CT in the imaging assessment of tumor multiplicity [26].

In both CT and MRI dynamic imaging studies, the assessment of tumor size and the detection of satellite nodules in iCCA typically involve the use of the portal venous phase [26,33]. Regarding MRI, hepatobiliary phase and diffusion-weighted imaging are also useful, particularly for detecting small lesions [34,35].

Vascular invasion: Vascular invasion, which includes both macrovascular invasion (MaVI) and microvascular invasion (MiVI) observed on histopathologic examination, is a major prognostic factor for iCCA. Specifically, it assigns a stage of T2 in the eighth edition AJCC system [22]. Research indicates that MiVI in iCCA is significantly linked to poor overall survival. Additionally, MaVI has been associated with comparatively low overall and disease-free survival [36,37].

The challenge of clinical staging arises from the inability to directly observe MiVI using CT or MRI. To address this issue, recent research has focused on identifying imaging characteristics that can predict the presence of MiVI in iCCA. Studies have found that MiVI is more commonly associated with larger tumors, lobulated or irregular tumor morphology, thin-rim enhancement during the arterial phase, penetration of the hepatic artery within the tumor, bile duct dilation, and a high apparent diffusion coefficient (ADC) [38-40].

Lymph node metastasis: Lymph node metastasis is widely recognized as a strong prognostic factor for iCCA [31,41]. The conventional criteria for detecting lymph node metastasis on CT and MRI generally involve a lymph node size threshold of 1 cm in short-axis diameter, along with imaging characteristics such as

round shape, irregular margins, and internal necrosis [42]. Recent studies have demonstrated that the inclusion of tumor imaging factors—such as arterial phase hypoenhancement, tumor multiplicity, bile duct involvement, periductal infiltrating growth pattern, and a primary tumor located in the left lobe—combined with serum tumor markers like elevated carcinoembryonic antigen (CEA) and carbohydrate antigen 19-9 (CA19-9) levels, can improve the accuracy of lymph node metastasis detection in iCCA [43-46].

However, the diagnostic accuracy of CT and MRI for detecting lymph node metastases is generally considered to be inadequate. The most recent EASL-ILCA guidelines advise the routine use of 18-fludeoxyglucose positron emission tomography-computed tomography (^{18}F-FDG PET-CT) for patients with apparently resectable iCCA to achieve precise clinical nodal staging [2]. This recommendation stems from a recent meta-analysis, which revealed that MRI has a sensitivity of 64% and a specificity of 69% for identifying lymph node metastases. In contrast, ^{18}F-FDG PET-CT demonstrated a sensitivity of 52% but a notably higher specificity of 92% [47].

Radiological prognosis prediction

Subclassification of iCCA: Subclassifying iCCA based on radiological findings can be useful for predicting prognosis, as LD-iCCA is associated with a poorer prognosis than SD-iCCA. Imaging can be employed to assess the differences in gross morphology between these types of iCCA. SD-iCCA typically exhibits a mass-forming appearance with a round or lobulated shape **(Figs. 1 and 2)** [48]. In contrast, LD-iCCA often displays irregular contours alongside a round or lobulated shape, frequent bile duct involvement that is readily apparent on T2-weighted MRI, and vascular encasement **(Fig. 3)** [9,10,48]. Recent studies indicate that features such as infiltrative contours, adjacent bile duct dilatation, the absence of arterial phase hyperenhancement, and vascular invasion are associated with LD-iCCA and are correlated with poorer disease-free and overall survival [48,49].

The imaging findings of the two types of iCCA closely align with their pathogenesis and associated liver or bile duct diseases. SD-iCCA is frequently accompanied by chronic hepatitis or cirrhosis, whereas LD-

iCCA is commonly associated with chronic bile duct conditions such as primary sclerosing cholangitis, hepatolithiasis, or *Clonorchis sinensis* infection [50-53].

Enhancement pattern of the tumor: The arterial enhancement pattern of iCCA is recognized as a key imaging-based prognostic marker. Studies have shown that iCCA with arterial phase hyperenhancement is associated with less invasive histopathological features and better overall survival compared to iCCA with either diffuse hypoenhancement or rim enhancement during the arterial phase **(Fig. 1)** [54-56]. Radiopathologic correlation studies have additionally established that MVD is linked to arterial enhancement patterns. iCCA with low MVD typically displays low arterial phase enhancement on imaging; furthermore, low MVD is associated with a poor prognosis, along with aggressive pathological features such as tumor multiplicity, MiVI, lymph node metastasis, and low infiltration of CD8+ tumor-infiltrating lymphocytes [57,58].

Moreover, the enhancement pattern of iCCA is suspected to be associated with its subclassification. SD-iCCA often exhibits arterial hyperenhancement, resembling that seen in HCC or combined hepatocellular-cholangiocarcinoma [59]. The arterial enhancement patterns in LD-iCCA are more variable, ranging from diffuse hyperenhancement to rim hyperenhancement and diffuse hypoenhancement [48].

Intratumoral fibrous stroma: Most iCCAs exhibit some degree of fibrous stroma. When scirrhous fibrous stroma comprises more than 70% of the tumor area, the iCCA is classified as scirrhous. Scirrhous iCCA is linked to a higher incidence of lymphatic and perineural invasion and is associated with significantly worse survival outcomes compared to non-scirrhous iCCA [60].

Intratumoral fibrosis can be assessed using dynamic CT or MRI. Radiopathologic correlation studies have demonstrated that regions of delayed enhancement are indicative of contrast retention within the fibrous stroma of the tumor [61-63]. Furthermore, the degree of delayed enhancement has been recognized as a prognostic marker for poor outcomes in patients with MF-iCCA. Specifically, iCCAs that exhibit delayed enhancement in more than two-thirds of the tumor on dynamic CT are associated with scirrhous iCCA, a higher incidence of perineural invasion, and relatively low overall survival [64].

Similarly, on gadoxetic acid-enhanced MRI, central intratumoral enhancement observed during the hepatobiliary phase reflects the presence of fibrous stroma within an iCCA lesion **(Fig. 4)** [65,66]. During this phase, iCCAs containing fibrous stroma exhibit an ill-defined hyperintense region set against a peripheral hypointense area. This pattern is often described as the "EOB-cloud," a term derived from the chemical name of gadoxetic acid, gadolinium ethoxybenzyl diethylenetriamine pentaacetic acid (Gd-EOB-DTPA) [66,67]. This cloud-like appearance results from the extracellular accumulation of contrast in the central fibrous stroma, while the periphery of the tumor typically contains a higher proportion of tumor tissue and less fibrosis. Notably, MF-iCCAs in which more than 50% of the area appears hyperintense or isointense during the hepatobiliary phase tend to exhibit comparatively poor disease-free and overall survival [68].

Imaging-based prognosis prediction model for iCCA

Recent research has progressed from correlating imaging findings with histopathologic characteristics associated with prognosis to creating models that directly predict prognosis from imaging data. These imaging-based prognostic models can offer insights into patient outcomes before treatment is initiated, potentially informing critical decisions about therapeutic strategies.

A multicenter study proposed a preoperative prognostic model for resectable iCCA that includes serum CA19-9 levels and three MRI findings: tumor multiplicity, lymph node metastasis, and bile duct invasion [69]. In predicting overall survival, this imaging-based model demonstrated comparable discriminatory performance to traditional pathologic staging systems, such as the eighth edition AJCC TNM system, the MEGNA score, and Nathan staging [69-71]. Another recent study introduced a more sophisticated prognostic model for resectable iCCA, combining two serum markers (CA19-9 >300 IU/mL and albumin ≤40 g/L) and six imaging findings [72]. This model outperformed pathologic staging systems, including the eighth edition AJCC and the MEGNA score, in predicting disease-specific and disease-free survival [72].

Imaging-based models have also been reported for predicting the prognosis of unresectable iCCA. The Fudan score, originally developed from a cohort of patients with resectable iCCA, has been shown to be

effective for prognostic prediction in unresectable iCCA as well [73]. This score includes five variables: tumor diameter, the number of intrahepatic tumors, the type of tumor boundary, serum alkaline phosphatase levels, and CA19-9 levels. A recent study proposed a modified scoring system for unresectable iCCA by incorporating an additional unfavorable prognostic factor—high ADC—which improved the model's performance in predicting survival [74].

Utilizing imaging findings for treatment decision-making in iCCA

Imaging is vital in the treatment decision-making process for iCCA, as it aids not only in assessing resectability but also in determining the need for lymphadenectomy during hepatic resection, deciding whether to administer neoadjuvant therapy, and selecting targeted therapies.

Lymphadenectomy

Lymphadenectomy plays a crucial role in accurate staging and may reduce the risk of recurrence; however, its impact on survival remains unclear. Although the practice of lymph node dissection in patients with clinically positive lymph nodes (cN+) has gained broader acceptance, the routine dissection of lymph nodes in patients who lack clear evidence of lymph node metastases (clinically negative lymph nodes, cN−) remains a topic of ongoing debate [75,76].

The AJCC staging system, EASL-ILCA guidelines, and National Comprehensive Cancer Network (NCCN) clinical practice guidelines all endorse the routine dissection of lymph nodes. The AJCC and EASL-ILCA guidelines specifically recommend the removal of a minimum of six lymph nodes to ensure thorough nodal staging. In comparison, the NCCN document simply advises regional lymphadenectomy of the porta hepatis [2,22,77]. Conversely, Japanese guidelines do not provide a specific recommendation concerning routine lymph node dissection [78].

In clinical practice, lymph node dissection is performed in about half of patients, largely based on the surgeon's discretion [79,80]. When deciding whether to perform lymph node dissection, imaging findings play a key role. One study revealed that a risk score combining serum CEA level (≥7 ng/mL), lymph nodes deemed suspicious on MRI, and MRI evidence of bile duct invasion was significantly correlated with the

presence of pathological lymph node metastasis **(Fig. 5)** [46]. Moreover, among patients who had a high risk score but did not undergo lymph node dissection, the researchers observed a higher likelihood of nodal recurrence within 3 months after surgery [46]. Imaging results can therefore be instrumental in stratifying the risk of lymph node metastasis, thus guiding the decision of whether to perform lymph node dissection in patients at high risk.

Neoadjuvant therapy

Currently, the literature includes no prospective evidence specifically supporting neoadjuvant therapy for iCCA, and no randomized studies have directly compared neoadjuvant chemotherapy followed by surgery with surgery alone. However, two retrospective studies, both analyzing data from the US National Cancer Database, yielded notable findings.

One study demonstrated that patients with a higher clinical T stage or clinical lymph node metastasis who received neoadjuvant therapy had better survival outcomes than those who underwent upfront surgery [81]. Similarly, another study found that although no survival benefit was observed in a propensity score-matched analysis across all stages of iCCA, neoadjuvant therapy did confer a survival advantage in patients with more advanced disease (stages II-III) [82].

As a result, guidelines vary in their recommendations concerning neoadjuvant therapy for iCCA. The EASL-ILCA publication states that neoadjuvant systemic chemotherapy can be considered for patients with surgically challenging yet resectable disease, especially when an R1 resection is anticipated [2]. In contrast, neither the NCCN nor the Japanese guidelines provide specific recommendations for neoadjuvant therapy in the context of iCCA [77,78]. Well-designed prospective trials are necessary to further evaluate the role of neoadjuvant treatment in this context.

Collectively, neoadjuvant therapy has been demonstrated to confer a survival benefit in cases with a high T stage, suspected nodal metastasis, or a high likelihood of positive resection margins. Considering that imaging-based prognostic models are highly effective at predicting postoperative outcomes, the use of imaging to identify high-risk patients who might benefit from neoadjuvant therapy could represent a viable strategy [72].

Molecular profiling for targeted therapy

In recent years, targeted therapy has become increasingly important in the treatment of iCCA [83]. The standard first-line treatment consists of a combination of gemcitabine, cisplatin, and durvalumab. However, targeted therapies are emerging as a viable second-line option for patients with specific genetic mutations [2,77]. These therapies require molecular profiling, often performed through next-generation sequencing, which can be expensive. Molecular profiling is typically recommended for patients with advanced-stage disease who need systemic therapy and for early-stage patients at high risk of recurrence. Imaging findings can be instrumental in identifying and stratifying these high-risk patients.

Currently, approved targeted therapies are available for genetic factors including isocitrate dehydrogenase 1 (*IDH1*) mutation, fibroblast growth factor receptor 2 (*FGFR2*) fusion, *BRAF* V600E mutation, microsatellite instability-high and mismatch repair-deficient cancers, and epidermal growth factor receptor 2 (*HER2*) overexpression [84-88]. Among these, *IDH1* mutation and *FGFR2* fusion are particularly impactful due to their comparatively high incidence [77]. These mutations are predominantly observed in SD-iCCA [18]. Studies have shown that iCCA with *IDH1/2* mutations often presents with pronounced arterial phase enhancement on imaging, a feature commonly associated with SD-iCCA [89]. Given the higher prevalence of targetable mutations such as *IDH1* and *FGFR2* within the small duct type, molecular profiling may be particularly promising when imaging findings suggest the presence of SD-iCCA **(Fig. 6)**. However, limited research is available to support this recommendation.

Conclusion

iCCA represents a serious and escalating global health concern, with a rising incidence and persistently poor prognosis. However, advancements in pathology and radiology have provided new insights into the disease. The histological subclassification into SD-iCCA and LD-iCCA offers a valuable framework for understanding the heterogeneity of iCCA and improving prognosis prediction. Radiological studies that focus on various imaging findings, such as tumor size, multiplicity, enhancement patterns, the presence of

intratumoral fibrous stroma, and suspicious lymph nodes, have demonstrated high utility in the pre-treatment assessment of patients.

Importantly, imaging-based prognostic models for resectable iCCA have demonstrated predictive accuracy comparable to that of traditional pathological staging systems. Beyond predicting prognosis, imaging also offers critical insights that may inform decisions about lymphadenectomy and neoadjuvant therapy. Furthermore, radiological findings indicative of SD-iCCA could assist in identifying patients likely to harbor clinically relevant mutations, such as *IDH1* mutations and *FGFR2* fusions.

These imaging-based approaches are essential for improving prognosis and tailoring treatment strategies for patients with iCCA, thereby advancing personalized medicine in this area. Nevertheless, to increase the utilization of imaging findings in predicting prognosis and informing treatment decisions, higher-level evidence from international multicenter prospective studies is necessary.

ORCID

Jun Gu Kang: https://orcid.org/0000-0002-9275-3194

Taek Chung: https://orcid.org/0000-0001-7567-0680

Dong Kyu Kim: https://orcid.org/0000-0001-7322-2550

Hyungjin Rhee: https://orcid.org/0000-0001-7759-4458

Authors' contribution

Project administration: Rhee H

Conceptualization: Rhee H

Methodology & data curation: Kang JG, Chung T, Kim DK, Rhee H

Funding acquisition: Rhee H

Writing – original draft: Kang JG, Rhee H

Writing – review & editing: Kang JG, Chung T, Kim DK

Funding

This work was supported by the National Research Foundation of Korea (NRF) grant funded by the Korea government (MSIT) (No. RS-2023-00208307).

Data availability

Not applicable.

Acknowledgments

Not applicable.

Supplementary materials

Not applicable.

References

1. Banales JM, Cardinale V, Carpino G, Marzioni M, Andersen JB, Invernizzi P, et al. Expert consensus document: Cholangiocarcinoma: current knowledge and future perspectives consensus statement from the European Network for the Study of Cholangiocarcinoma (ENS-CCA). *Nat Rev Gastroenterol Hepatol* 2016;13(5):261-280.
2. European Association for the Study of the Liver. Electronic address eee, European Association for the Study of the L. EASL-ILCA Clinical Practice Guidelines on the management of intrahepatic cholangiocarcinoma. *J Hepatol* 2023;79(1):181-208.
3. Banales JM, Marin JJG, Lamarca A, Rodrigues PM, Khan SA, Roberts LR, et al. Cholangiocarcinoma 2020: the next horizon in mechanisms and management. *Nat Rev Gastroenterol Hepatol* 2020;17(9):557-588.
4. Yang JQ, Wang XG, Wu B. Incidence trend and prognosis of intrahepatic cholangiocarcinoma: a study based on the SEER database. *Transl Cancer Res* 2023;12(11):3007-3015.

5. Seo N, Kim DY, Choi JY. Cross-Sectional Imaging of Intrahepatic Cholangiocarcinoma: Development, Growth, Spread, and Prognosis. *AJR Am J Roentgenol* 2017;209(2):W64-W75.

6. Zhang Y, Uchida M, Abe T, Nishimura H, Hayabuchi N, Nakashima Y. Intrahepatic peripheral cholangiocarcinoma: comparison of dynamic CT and dynamic MRI. *J Comput Assist Tomogr* 1999;23(5):670-677.

7. Kang Y, Lee JM, Kim SH, Han JK, Choi BI. Intrahepatic mass-forming cholangiocarcinoma: enhancement patterns on gadoxetic acid-enhanced MR images. *Radiology* 2012;264(3):751-760.

8. Maetani Y, Itoh K, Watanabe C, Shibata T, Ametani F, Yamabe H, et al. MR imaging of intrahepatic cholangiocarcinoma with pathologic correlation. *AJR Am J Roentgenol* 2001;176(6):1499-1507.

9. Nam JG, Lee JM, Joo I, Ahn SJ, Park JY, Lee KB, et al. Intrahepatic Mass-Forming Cholangiocarcinoma: Relationship Between Computed Tomography Characteristics and Histological Subtypes. *J Comput Assist Tomogr* 2018;42(3):340-349.

10. Rhee H, Kim MJ, Park YN, An C. A proposal of imaging classification of intrahepatic mass-forming cholangiocarcinoma into ductal and parenchymal types: clinicopathologic significance. *Eur Radiol* 2019;29(6):3111-3121.

11. Bosman, F. T., Carneiro, F., Hruban, R. & Theise N. WHO Classification of Tumours: Digestive System Tumours 5th edn Vol. 1 (IARC, 2019).

12. Komuta M. Intrahepatic cholangiocarcinoma: histological diversity and the role of the pathologist. *J Liver Cancer* 2024;24(1):17-22.

13. Nakanuma Y, Sato Y, Harada K, Sasaki M, Xu J, Ikeda H. Pathological classification of intrahepatic cholangiocarcinoma based on a new concept. *World J Hepatol* 2010;2(12):419-427.

14. Aishima S, Oda Y. Pathogenesis and classification of intrahepatic cholangiocarcinoma: different characters of perihilar large duct type versus peripheral small duct type. *J Hepatobiliary Pancreat Sci* 2015;22(2):94-100.

15. Jeon Y, Kwon SM, Rhee H, Yoo JE, Chung T, Woo HG, et al. Molecular and radiopathologic spectrum between HCC and intrahepatic cholangiocarcinoma. *Hepatology* 2023;77(1):92-108.

16. Chung T, Rhee H, Nahm JH, Jeon Y, Yoo JE, Kim YJ, et al. Clinicopathological characteristics of intrahepatic cholangiocarcinoma according to gross morphologic type: cholangiolocellular differentiation traits and inflammation- and proliferation-phenotypes. *HPB (Oxford)* 2020;22(6):864-873.

17. Nakanuma Y, Sasaki M, Sato Y, Ren X, Ikeda H, Harada K. Multistep carcinogenesis of perihilar cholangiocarcinoma arising in the intrahepatic large bile ducts. *World J Hepatol* 2009;1(1):35-42.

18. Chung T, Park YN. Up-to-Date Pathologic Classification and Molecular Characteristics of Intrahepatic Cholangiocarcinoma. *Front Med (Lausanne)* 2022;9:857140.

19. Li Z, Nguyen Canh H, Takahashi K, Le Thanh D, Nguyen Thi Q, Yang R, et al. Histopathological growth pattern and vessel co-option in intrahepatic cholangiocarcinoma. *Med Mol Morphol* 2024;57(3):200-217.

20. Sugita H, Nakanuma S, Gabata R, Tokoro T, Takei R, Okazaki M, et al. Clinicopathological features of cholangiolocarcinoma and impact of tumor heterogeneity on prognosis: A single institution retrospective study. *Oncol Lett* 2024;27(5):213.

21. Hayashi A, Misumi K, Shibahara J, Arita J, Sakamoto Y, Hasegawa K, et al. Distinct Clinicopathologic and Genetic Features of 2 Histologic Subtypes of Intrahepatic Cholangiocarcinoma. *Am J Surg Pathol* 2016;40(8):1021-1030.

22. Amin MB, Greene FL, Edge SB, Compton CC, Gershenwald JE, Brookland RK, et al. The Eighth Edition AJCC Cancer Staging Manual: Continuing to build a bridge from a population-based to a more "personalized" approach to cancer staging. *CA Cancer J Clin* 2017;67(2):93-99.

23. Kim Y, Moris DP, Zhang XF, Bagante F, Spolverato G, Schmidt C, et al. Evaluation of the 8th edition American Joint Commission on Cancer (AJCC) staging system for patients with intrahepatic cholangiocarcinoma: A surveillance, epidemiology, and end results (SEER) analysis. *J Surg Oncol* 2017;116(6):643-650.

24. Spolverato G, Bagante F, Weiss M, Alexandrescu S, Marques HP, Aldrighetti L, et al. Comparative performances of the 7th and the 8th editions of the American Joint Committee on Cancer staging systems for intrahepatic cholangiocarcinoma. *J Surg Oncol* 2017;115(6):696-703.

25. Kang SH, Hwang S, Lee YJ, Kim KH, Ahn CS, Moon DB, et al. Prognostic comparison of the 7th and 8th editions of the American Joint Committee on Cancer staging system for intrahepatic cholangiocarcinoma. *J Hepatobiliary Pancreat Sci* 2018;25(4):240-248.

26. Kim YY, Yeom SK, Shin H, Choi SH, Rhee H, Park JH, et al. Clinical Staging of Mass-Forming Intrahepatic Cholangiocarcinoma: Computed Tomography Versus Magnetic Resonance Imaging. *Hepatol Commun* 2021;5(12):2009-2018.

27. Hyder O, Hatzaras I, Sotiropoulos GC, Paul A, Alexandrescu S, Marques H, et al. Recurrence after operative management of intrahepatic cholangiocarcinoma. *Surgery* 2013;153(6):811-818.

28. Ali SM, Clark CJ, Mounajjed T, Wu TT, Harmsen WS, Reid-Lombardo KM, et al. Model to predict survival after surgical resection of intrahepatic cholangiocarcinoma: the Mayo Clinic experience. *HPB (Oxford)* 2015;17(3):244-250.

29. Hwang S, Lee YJ, Song GW, Park KM, Kim KH, Ahn CS, et al. Prognostic Impact of Tumor Growth Type on 7th AJCC Staging System for Intrahepatic Cholangiocarcinoma: a Single-Center Experience of 659 Cases. *J Gastrointest Surg* 2015;19(7):1291-1304.

30. Doussot A, Gonen M, Wiggers JK, Groot-Koerkamp B, DeMatteo RP, Fuks D, et al. Recurrence Patterns and Disease-Free Survival after Resection of Intrahepatic Cholangiocarcinoma: Preoperative and Postoperative Prognostic Models. *J Am Coll Surg* 2016;223(3):493-505 e492.

31. Mavros MN, Economopoulos KP, Alexiou VG, Pawlik TM. Treatment and Prognosis for Patients With Intrahepatic Cholangiocarcinoma: Systematic Review and Meta-analysis. *JAMA Surg* 2014;149(6):565-574.

32. Tabrizian P, Jibara G, Hechtman JF, Franssen B, Labow DM, Schwartz ME, et al. Outcomes following resection of intrahepatic cholangiocarcinoma. *HPB (Oxford)* 2015;17(4):344-351.

33. Olthof SC, Othman A, Clasen S, Schraml C, Nikolaou K, Bongers M. Imaging of Cholangiocarcinoma. *Visc Med* 2016;32(6):402-410.

34. Peporte AR, Sommer WH, Nikolaou K, Reiser MF, Zech CJ. Imaging features of intrahepatic cholangiocarcinoma in Gd-EOB-DTPA-enhanced MRI. *Eur J Radiol* 2013;82(3):e101-106.

35. Marion-Audibert AM, Vullierme MP, Ronot M, Mabrut JY, Sauvanet A, Zins M, et al. Routine MRI With DWI Sequences to Detect Liver Metastases in Patients With Potentially Resectable Pancreatic Ductal Carcinoma and Normal Liver CT: A Prospective Multicenter Study. *AJR Am J Roentgenol* 2018;211(5):W217-W225.

36. Shao C, Chen J, Chen J, Shi J, Huang L, Qiu Y. Histological classification of microvascular invasion to predict prognosis in intrahepatic cholangiocarcinoma. *Int J Clin Exp Pathol* 2017;10(7):7674-7681.

37. Hu LS, Weiss M, Popescu I, Marques HP, Aldrighetti L, Maithel SK, et al. Impact of microvascular invasion on clinical outcomes after curative-intent resection for intrahepatic cholangiocarcinoma. *J Surg Oncol* 2019;119(1):21-29.

38. Zhou Y, Wang X, Xu C, Zhou G, Liu X, Gao S, et al. Mass-forming intrahepatic cholangiocarcinoma: Can diffusion-weighted imaging predict microvascular invasion? *J Magn Reson Imaging* 2019;50(1):315-324.

39. Ma X, Liu L, Fang J, Rao S, Lv L, Zeng M, et al. MRI features predict microvascular invasion in intrahepatic cholangiocarcinoma. *Cancer Imaging* 2020;20(1):40.

40. Zhou Y, Zhou G, Zhang J, Xu C, Wang X, Xu P. Radiomics signature on dynamic contrast-enhanced MR images: a potential imaging biomarker for prediction of microvascular invasion in mass-forming intrahepatic cholangiocarcinoma. *Eur Radiol* 2021;31(9):6846-6855.

41. Kawarada Y, Yamagiwa K, Das BC. Analysis of the relationships between clinicopathologic factors and survival time in intrahepatic cholangiocarcinoma. *Am J Surg* 2002;183(6):679-685.

42. Ganeshalingam S, Koh DM. Nodal staging. *Cancer Imaging* 2009;9(1):104-111.

43. Yamamoto Y, Turkoglu MA, Aramaki T, Sugiura T, Okamura Y, Ito T, et al. Vascularity of Intrahepatic Cholangiocarcinoma on Computed Tomography is Predictive of Lymph Node Metastasis. *Ann Surg Oncol* 2016;23(Suppl 4):485-493.

44. Meng ZW, Lin XQ, Zhu JH, Han SH, Chen YL. A nomogram to predict lymph node metastasis before resection in intrahepatic cholangiocarcinoma. *J Surg Res* 2018;226:56-63.

45. Tsilimigras DI, Sahara K, Paredes AZ, Moro A, Mehta R, Moris D, et al. Predicting Lymph Node Metastasis in Intrahepatic Cholangiocarcinoma. *J Gastrointest Surg* 2021;25(5):1156-1163.

46. Rhee H, Lim HJ, Han K, Yeom SK, Choi SH, Park JH, et al. A preoperative scoring system to predict lymph node metastasis in intrahepatic cholangiocarcinoma. *Hepatol Int* 2023;17(4):942-953.

47. Huang X, Yang J, Li J, Xiong Y. Comparison of magnetic resonance imaging and 18-fludeoxyglucose positron emission tomography/computed tomography in the diagnostic accuracy of staging in patients with cholangiocarcinoma: A meta-analysis. *Medicine (Baltimore)* 2020;99(35):e20932.

48. Park S, Lee Y, Kim H, Yu MH, Lee ES, Yoon JH, et al. Subtype Classification of Intrahepatic Cholangiocarcinoma Using Liver MR Imaging Features and Its Prognostic Value. *Liver Cancer* 2022;11(3):233-246.

49. Park M-S. Review of Mass-Forming Intrahepatic Cholangiocarcinoma. *Korean Journal of Abdominal Radiology* 2022;6(1):1-11.

50. Zen Y. Intrahepatic cholangiocarcinoma: typical features, uncommon variants, and controversial related entities. *Hum Pathol* 2023;132:197-207.

51. Giambelluca D, Cutaia G, Midiri M, Salvaggio G. The "pruned tree" appearance of primary sclerosing cholangitis. *Abdom Radiol (NY)* 2019;44(8):2935-2936.

52. Giambelluca D, Leto C, D'Arpa F, Midiri M, Salvaggio G. Beaded bile ducts in primary sclerosing cholangitis. *Abdom Radiol (NY)* 2019;44(3):1195-1196.

53. Lim JH. Liver flukes: the malady neglected. *Korean J Radiol* 2011;12(3):269-279.

54. Ariizumi S, Kotera Y, Takahashi Y, Katagiri S, Chen IP, Ota T, et al. Mass-forming intrahepatic cholangiocarcinoma with marked enhancement on arterial-phase computed tomography reflects favorable surgical outcomes. *J Surg Oncol* 2011;104(2):130-139.

55. Nanashima A, Abo T, Murakami G, Matsumoto A, Tou K, Takeshita H, et al. Intrahepatic cholangiocarcinoma: relationship between tumor imaging enhancement by measuring attenuation and clinicopathologic characteristics. *Abdom Imaging* 2013;38(4):785-792.

56. Min JH, Kim YK, Choi SY, Kang TW, Lee SJ, Kim JM, et al. Intrahepatic Mass-forming Cholangiocarcinoma: Arterial Enhancement Patterns at MRI and Prognosis. *Radiology* 2019;290(3):691-699.

57. Yugawa K, Itoh S, Yoshizumi T, Iseda N, Tomiyama T, Toshima T, et al. Prognostic impact of tumor microvessels in intrahepatic cholangiocarcinoma: association with tumor-infiltrating lymphocytes. *Mod Pathol* 2021;34(4):798-807.

58. Vigano L, Soldani C, Franceschini B, Cimino M, Lleo A, Donadon M, et al. Tumor-Infiltrating Lymphocytes and Macrophages in Intrahepatic Cholangiocellular Carcinoma. Impact on Prognosis after Complete Surgery. *J Gastrointest Surg* 2019;23(11):2216-2224.

59. Rhee H, Park JH, Park YN. Update on Pathologic and Radiologic Diagnosis of Combined Hepatocellular-Cholangiocarcinoma. *J Liver Cancer* 2021;21(1):12-24.

60. Kajiyama K, Maeda T, Takenaka K, Sugimachi K, Tsuneyoshi M. The significance of stromal desmoplasia in intrahepatic cholangiocarcinoma: a special reference of 'scirrhous-type' and 'nonscirrhous-type' growth. *Am J Surg Pathol* 1999;23(8):892-902.

61. Lacomis JM, Baron RL, Oliver JH, 3rd, Nalesnik MA, Federle MP. Cholangiocarcinoma: delayed CT contrast enhancement patterns. *Radiology* 1997;203(1):98-104.

62. Yoshikawa J, Matsui O, Kadoya M, Gabata T, Arai K, Takashima T. Delayed enhancement of fibrotic areas in hepatic masses: CT-pathologic correlation. *J Comput Assist Tomogr* 1992;16(2):206-211.

63. Valls C, Guma A, Puig I, Sanchez A, Andia E, Serrano T, et al. Intrahepatic peripheral cholangiocarcinoma: CT evaluation. *Abdom Imaging* 2000;25(5):490-496.

64. Asayama Y, Yoshimitsu K, Irie H, Tajima T, Nishie A, Hirakawa M, et al. Delayed-phase dynamic CT enhancement as a prognostic factor for mass-forming intrahepatic cholangiocarcinoma. *Radiology* 2006;238(1):150-155.

65. Jeong HT, Kim MJ, Chung YE, Choi JY, Park YN, Kim KW. Gadoxetate disodium-enhanced MRI of mass-forming intrahepatic cholangiocarcinomas: imaging-histologic correlation. *AJR Am J Roentgenol* 2013;201(4):W603-611.

66. Kim SH, Lee CH, Kim BH, Kim WB, Yeom SK, Kim KA, et al. Typical and atypical imaging findings of intrahepatic cholangiocarcinoma using gadolinium ethoxybenzyl diethylenetriamine pentaacetic acid-enhanced magnetic resonance imaging. *J Comput Assist Tomogr* 2012;36(6):704-709.

67. Teo T, Chawla A. The cloud sign of mass-forming intrahepatic cholangiocarcinoma. *Abdom Radiol (NY)* 2020;45(1):237-238.

68. Koh J, Chung YE, Nahm JH, Kim HY, Kim KS, Park YN, et al. Intrahepatic mass-forming cholangiocarcinoma: prognostic value of preoperative gadoxetic acid-enhanced MRI. *Eur Radiol* 2016;26(2):407-416.

69. Rhee H, Choi SH, Park JH, Cho ES, Yeom SK, Park S, et al. Preoperative magnetic resonance imaging-based prognostic model for mass-forming intrahepatic cholangiocarcinoma. *Liver Int* 2022;42(4):930-941.

70. Nathan H, Aloia TA, Vauthey JN, Abdalla EK, Zhu AX, Schulick RD, et al. A proposed staging system for intrahepatic cholangiocarcinoma. *Ann Surg Oncol* 2009;16(1):14-22.

71. Raoof M, Dumitra S, Ituarte PHG, Melstrom L, Warner SG, Fong Y, et al. Development and Validation of a Prognostic Score for Intrahepatic Cholangiocarcinoma. *JAMA Surg* 2017;152(5):e170117.

72. Ji GW, Xu Q, Jiao CY, Lu M, Xu ZG, Zhang B, et al. Translating imaging traits of mass-forming intrahepatic cholangiocarcinoma into the clinic: From prognostic to therapeutic insights. *JHEP Rep* 2023;5(10):100839.

73. Jiang W, Zeng ZC, Tang ZY, Fan J, Sun HC, Zhou J, et al. A prognostic scoring system based on clinical features of intrahepatic cholangiocarcinoma: the Fudan score. *Ann Oncol* 2011;22(7):1644-1652.

74. Pandey A, Mohseni A, Shaghaghi M, Pandey P, Rezvani Habibabadi R, Hazhirkarzar B, et al. Incremental value of volumetric multiparametric MRI over Fudan score for prognosis of unresectable intrahepatic cholangiocarcinoma treated with systemic chemotherapy. *Eur J Radiol* 2024;170:111196.

75. Sposito C, Droz Dit Busset M, Virdis M, Citterio D, Flores M, Bongini M, et al. The role of lymphadenectomy in the surgical treatment of intrahepatic cholangiocarcinoma: A review. *Eur J Surg Oncol* 2022;48(1):150-159.

76. Sposito C, Ratti F, Cucchetti A, Ardito F, Ruzzenente A, Di Sandro S, et al. Survival benefit of adequate lymphadenectomy in patients undergoing liver resection for clinically node-negative intrahepatic cholangiocarcinoma. *J Hepatol* 2023;78(2):356-363.

77. NCCN Clinical Practice Guidelines in Oncology. Biliary Tract Cancers (Version 3.2024). https://www.nccn.org/professionals/physician_gls/pdf/btc.pdf. Accessed August 27, 2024.

78. Kubo S, Shinkawa H, Asaoka Y, Ioka T, Igaki H, Izumi N, et al. Liver Cancer Study Group of Japan Clinical Practice Guidelines for Intrahepatic Cholangiocarcinoma. *Liver Cancer* 2022;11(4):290-314.

79. Clark CJ, Wood-Wentz CM, Reid-Lombardo KM, Kendrick ML, Huebner M, Que FG. Lymphadenectomy in the staging and treatment of intrahepatic cholangiocarcinoma: a population-based study using the National Cancer Institute SEER database. *HPB (Oxford)* 2011;13(9):612-620.

80. Zhang XF, Chen Q, Kimbrough CW, Beal EW, Lv Y, Chakedis J, et al. Lymphadenectomy for Intrahepatic Cholangiocarcinoma: Has Nodal Evaluation Been Increasingly Adopted by Surgeons over Time?A National Database Analysis. *J Gastrointest Surg* 2018;22(4):668-675.

81. Mason MC, Massarweh NN, Tzeng CD, Chiang YJ, Chun YS, Aloia TA, et al. Time to Rethink Upfront Surgery for Resectable Intrahepatic Cholangiocarcinoma? Implications from the Neoadjuvant Experience. *Ann Surg Oncol* 2021;28(11):6725-6735.

82. Utuama O, Permuth JB, Dagne G, Sanchez-Anguiano A, Alman A, Kumar A, et al. Neoadjuvant Chemotherapy for Intrahepatic Cholangiocarcinoma: A Propensity Score Survival Analysis Supporting Use in Patients with High-Risk Disease. *Ann Surg Oncol* 2021;28(4):1939-1949.

83. Zanuso V, Tesini G, Valenzi E, Rimassa L. New systemic treatment options for advanced cholangiocarcinoma. *J Liver Cancer* 2024;24(2):155-170.

84. Abou-Alfa GK, Macarulla T, Javle MM, Kelley RK, Lubner SJ, Adeva J, et al. Ivosidenib in IDH1-mutant, chemotherapy-refractory cholangiocarcinoma (ClarIDHy): a multicentre, randomised, double-blind, placebo-controlled, phase 3 study. *Lancet Oncol* 2020;21(6):796-807.

85. Zhu AX, Macarulla T, Javle MM, Kelley RK, Lubner SJ, Adeva J, et al. Final Overall Survival Efficacy Results of Ivosidenib for Patients With Advanced Cholangiocarcinoma With IDH1 Mutation: The Phase 3 Randomized Clinical ClarIDHy Trial. *JAMA Oncol* 2021;7(11):1669-1677.

86. Goyal L, Meric-Bernstam F, Hollebecque A, Valle JW, Morizane C, Karasic TB, et al. Futibatinib for FGFR2-Rearranged Intrahepatic Cholangiocarcinoma. *N Engl J Med* 2023;388(3):228-239.

87. Abou-Alfa GK, Sahai V, Hollebecque A, Vaccaro G, Melisi D, Al-Rajabi R, et al. Pemigatinib for previously treated, locally advanced or metastatic cholangiocarcinoma: a multicentre, open-label, phase 2 study. *Lancet Oncol* 2020;21(5):671-684.

88. Maio M, Ascierto PA, Manzyuk L, Motola-Kuba D, Penel N, Cassier PA, et al. Pembrolizumab in microsatellite instability high or mismatch repair deficient cancers: updated analysis from the phase II KEYNOTE-158 study. *Ann Oncol* 2022;33(9):929-938.

89. Zhu Y, Chen J, Kong W, Mao L, Kong W, Zhou Q, et al. Predicting IDH mutation status of intrahepatic cholangiocarcinomas based on contrast-enhanced CT features. *Eur Radiol* 2018;28(1):159-169.

TABLES

Table 1. Comparison of characteristics between small duct and large duct iCCA

Characteristic	Small duct iCCA	Large duct iCCA
Location	Peripheral	Close to hilum
Etiology	Chronic hepatitis, cirrhosis	Hepatolithiasis, PSC
Postulated cell origin	Small bile duct, canal of Hering	Large bile duct, peribiliary gland
Shape of cancer cells	Low columnar to cuboidal	Columnar cells
Precursor lesions	(−)	(+ / BilIN, IPNB)
Gross morphology	Mass-forming (MF) type	Various
Perineural invasion	(+/−)	(++)
Lymphovascular invasion	(+/−)	(++)
Lymph node metastasis	(+/−)	(++)
Prognosis	Good	Poor
Molecular marker(s)	NCAM (+), N-cadherin (+)	S100P (+)
Mutation(s)	*IDH1/2* mutation, *FGFR2* fusion	*KRAS* mutation
Vasculature	Arteries (+), high MVD	Arteries (+/−), low MVD
Necrosis	(+/−)	(+)

iCCA, intrahepatic cholangiocarcinoma; PSC, primary sclerosing cholangitis; BilIN, biliary intraepithelial neoplasia; IPNB, intraductal papillary neoplasm of the bile duct; NCAM, neural cell adhesion molecule; N-cadherin, neural cadherin; IDH, isocitrate dehydrogenase; FGFR2, fibroblast growth factor receptor 2; KRAS, Kirsten rat sarcoma viral oncogene homolog; MVD, microvessel density.

FIGURE LEGENDS

Fig. 1. A 34-year-old female patient with liver cirrhosis and small duct-type intrahepatic cholangiocarcinoma (iCCA).

Gadoxetic acid-enhanced magnetic resonance imaging (MRI): (A) pre-contrast T1-weighted, (B) arterial phase, (C) portal phase, (D) transitional phase, (E) hepatobiliary phase, (F) T2-weighted, and (G) diffusion-weighted (b = 800 s/mm^2) images and (H) apparent diffusion coefficient map. Staining: (I) hematoxylin-eosin, (J) C-reactive protein (CRP) immunohistochemical, and (K) mucicarmine staining (I–K, original magnification ×200). The gadoxetic acid-enhanced MRI reveals a 1.5-cm round mass in the subcapsular area of the right liver. The mass exhibits hyperenhancement in the arterial phase (B), does not show washout in the portal phase (C), and appears hypointense in the hepatobiliary phase (E). Pathological examination confirmed the lesion as a small duct iCCA with positive CRP expression (J) and the absence of mucin under mucicarmine staining (K).

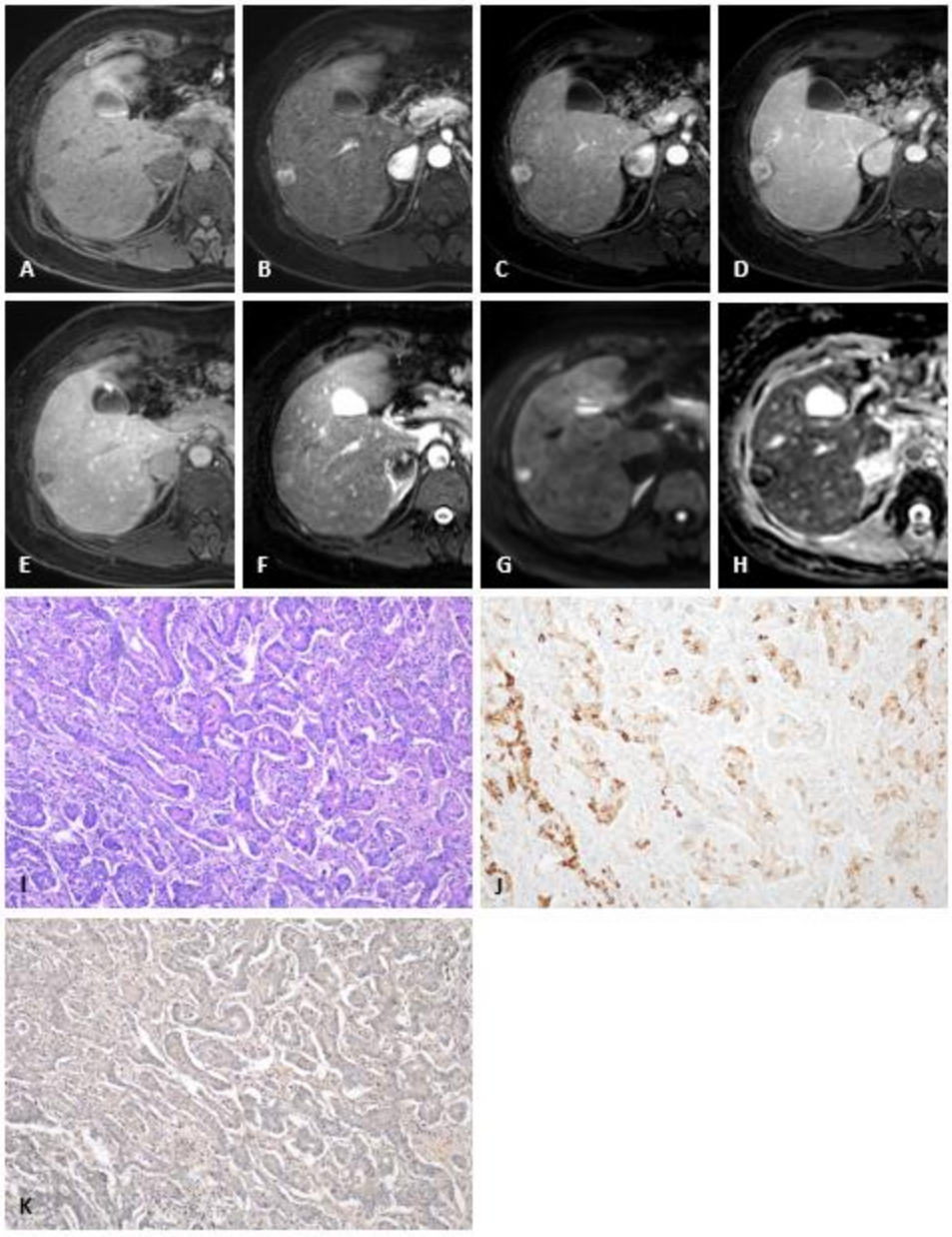
A
B
C
D
E
F
G
H
I
J
K

Fig. 2. A 51-year-old female patient with small duct-type intrahepatic cholangiocarcinoma (iCCA). Gadobutrol-enhanced magnetic resonance imaging: (A) pre-contrast T1-weighted, (B) arterial phase, (C) portal phase, (D) equilibrium phase, (E) 15-minute delayed phase, (F) T2-weighted, and (G) diffusion-weighted (b = 800 s/mm^2) images and (H) apparent diffusion coefficient (ADC) map. Staining: (I) hematoxylin-eosin, (J) C-reactive protein (CRP) immunohistochemical, (K) Alcian blue/periodic acid-Schiff (AB/PAS), and (L) S100 calcium-binding protein P (S100P) immunohistochemical staining (I–L, original magnification ×200). The mass exhibits rim hyperenhancement in the arterial phase (B) and a progressive centripetal pattern of contrast filling in the portal (C), equilibrium (D), and delayed (F) phases. It also displays moderate hyperintensity on the T2-weighted image (F), and restriction on both the diffusion-weighted image and the ADC map (G, H). No significant bile duct dilatation is evident in the peritumoral area. The patient underwent right lobectomy, and a diagnosis of small duct iCCA was confirmed through immunohistochemical and special staining techniques. Specifically, on pathologic examination, the lesion displayed positive CRP expression (J), absence of mucin on AB/PAS staining (K), and negative staining for S100P expression (L).

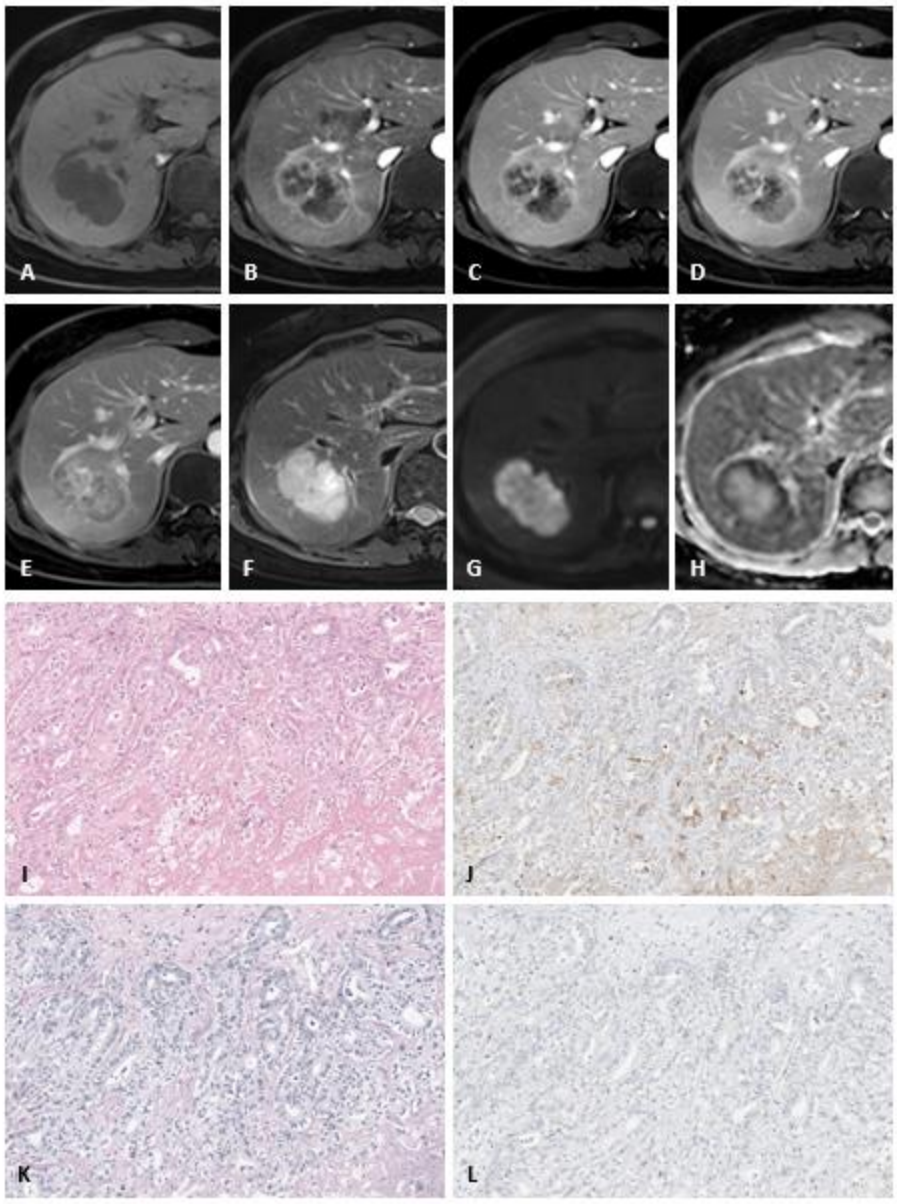
A
B
C
D
E
F
G
H
I
J
K
L

Fig. 3. A 52-year-old male patient with large duct-type intrahepatic cholangiocarcinoma (iCCA). Gadoxetic acid-enhanced magnetic resonance imaging: (A) pre-contrast T1-weighted, (B) arterial phase, (C) portal phase, (D) transitional phase, (E) hepatobiliary phase, (F) T2-weighted, and (G) diffusion-weighted (b = 800 s/mm^2) images and (H) apparent diffusion coefficient (ADC) map. Staining: (I) hematoxylin-eosin, (J) mucicarmine, and (K) S100 calcium-binding protein P (S100P) immunohistochemical staining (I–K, original magnification ×200). A well-defined 3.2-cm mass is evident in segment 4 of the liver. The mass exhibits diffuse hypovascularity in the arterial phase (B); hypointensity in the portal (C), transitional (D), and hepatobiliary phases (E); adjacent bile duct dilatation on the T2-weighted image (F); and restricted diffusion on both the diffusion-weighted image and the ADC map (G, H). The patient underwent percutaneous biopsy, and a diagnosis of large duct iCCA was confirmed through immunohistochemical and special staining techniques. Specifically, the tumor displayed positive expression of both mucin (J) and S100P (K).

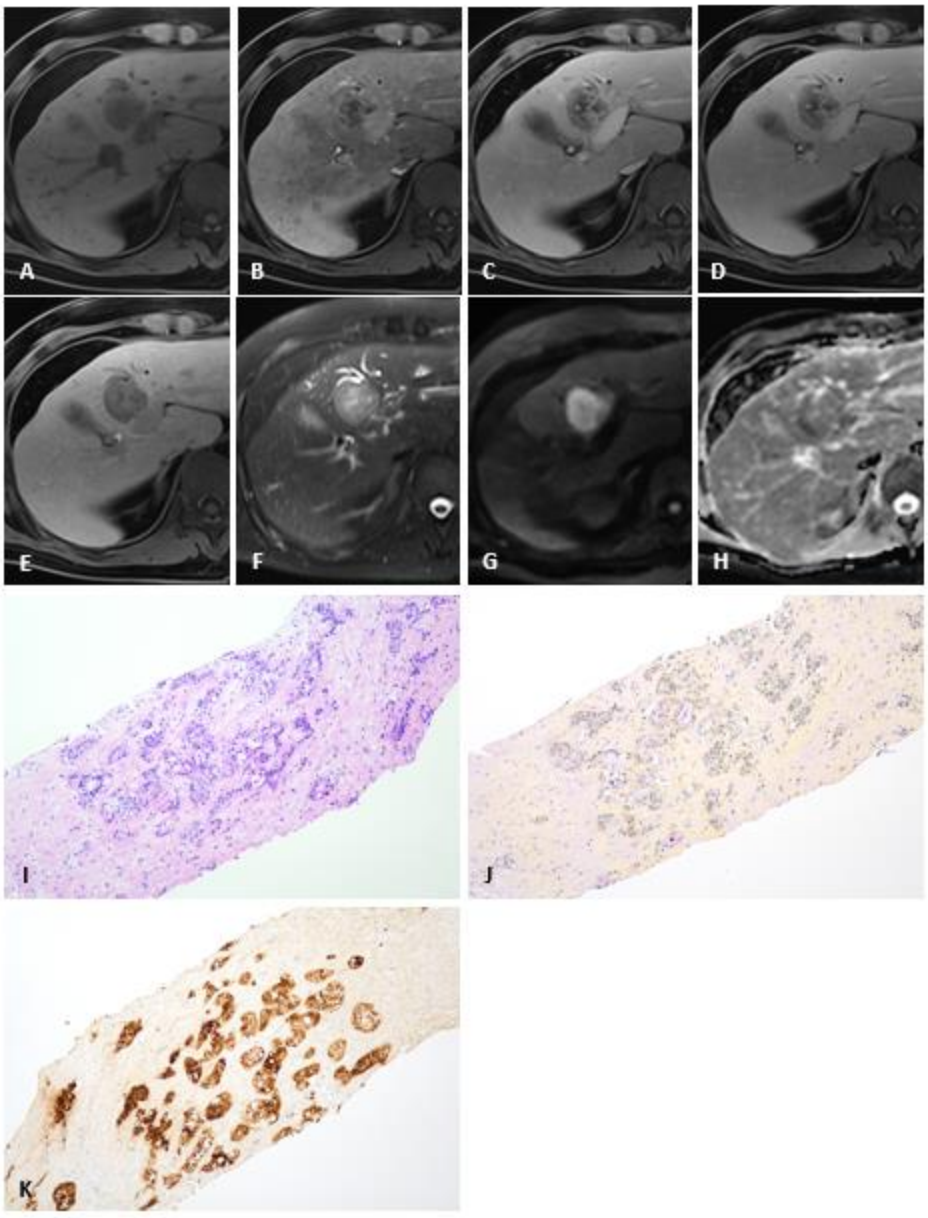
A
B
C
D
E
F
G
H
I
J
K

Fig. 4. A 63-year-old male patient with intrahepatic cholangiocarcinoma (iCCA) exhibiting a dense fibrous stroma.

Gadoxetic acid-enhanced magnetic resonance imaging (MRI): (A) pre-contrast T1-weighted, (B) arterial phase, (C) portal phase, (D) transitional phase, (E) hepatobiliary phase, (F) T2-weighted, and (G) diffusion-weighted (b = 800 s/mm^2) images and (H) apparent diffusion coefficient map. (I) ScanView image of hematoxylin-eosin staining. MRI revealed an approximately 4.5-cm lobulated mass in the right posterior liver. The mass exhibited thin-rim hyperenhancement in the arterial phase (B), peripheral washout with progressive central enhancement in the portal (C) and transitional (D) phases, and an "EOB-cloud" appearance in the hepatobiliary phase (E), as well as targetoid diffusion restriction (G, H). The patient underwent extended right posterior sectionectomy, and the diagnosis of iCCA was confirmed. The pathology specimen (I) displayed a dense fibrotic area, corresponding to the "EOB-cloud area" observed on MRI.

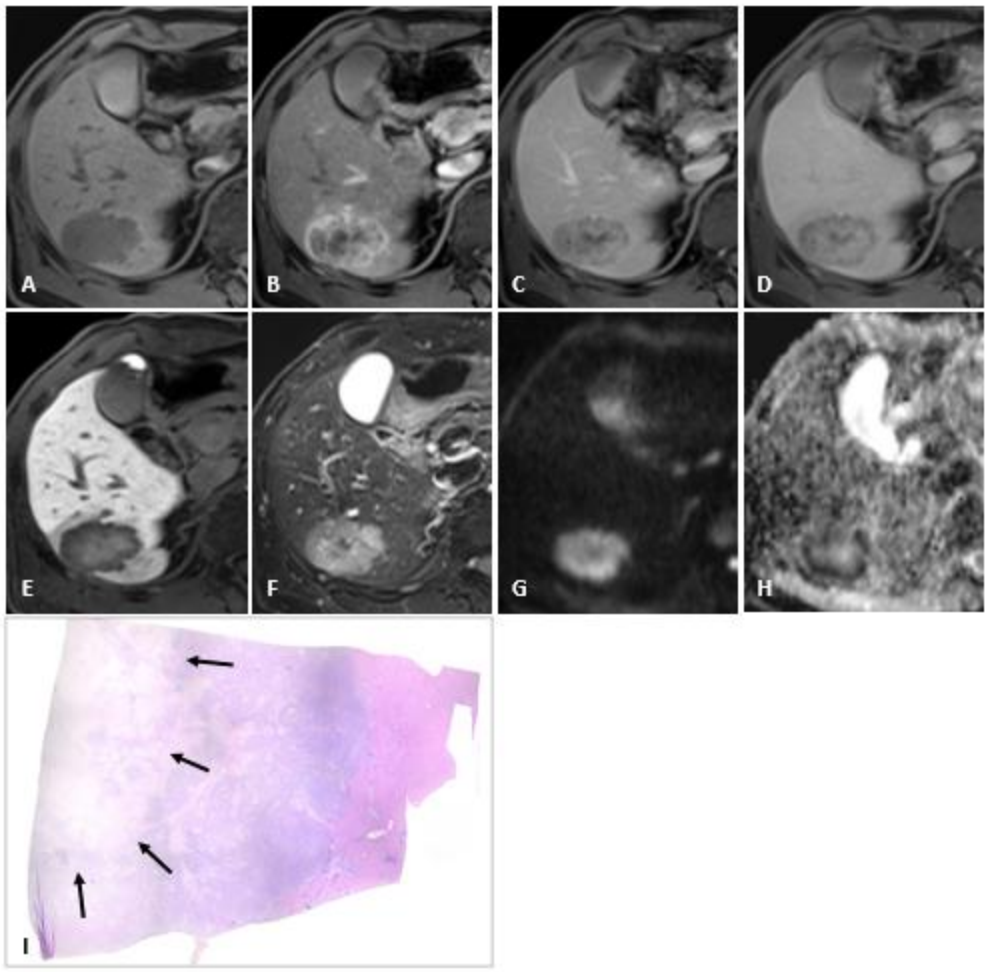
A
B
C
D
E
F
G
H
I

Fig. 5. A 64-year-old female patient with intrahepatic cholangiocarcinoma (iCCA) and lymph node metastasis.

Gadoxetic acid-enhanced magnetic resonance imaging, comprising (A) pre-contrast T1-weighted, (B) arterial phase, (C) portal phase, (D) hepatobiliary phase, (E) diffusion-weighted (b = 800 s/mm^2), and (F) T2-weighted images, reveals a 3.5-cm infiltrative, poorly enhancing mass in the left lobe, with adjacent bile duct dilatation. Additionally, the (G) portal phase image and (H) ^{18}F-fluorodeoxyglucose (^{18}F-FDG) positron emission tomography-computed tomography display an enlarged lymph node with increased ^{18}F-FDG uptake situated adjacent to the common hepatic artery (white arrows). The patient underwent left hepatic lobectomy with lymph node dissection, and pathological examination confirmed the diagnosis of iCCA with regional lymph node metastases.

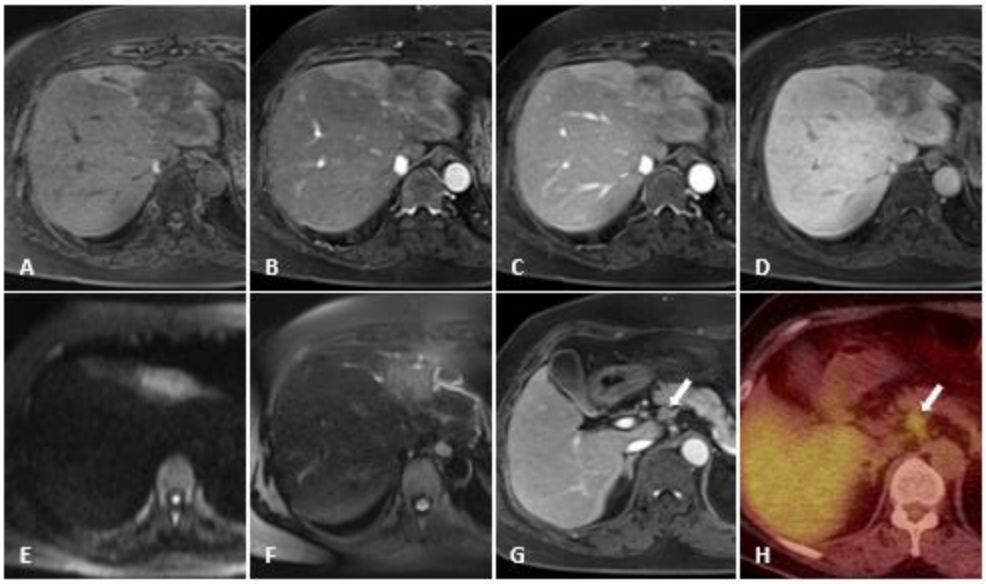

Fig. 6. A 42-year-old female patient with intrahepatic cholangiocarcinoma (iCCA) harboring an isocitrate dehydrogenase 1 (*IDH1*) mutation.

Gadoxetic acid-enhanced magnetic resonance imaging, comprising (A) pre-contrast T1-weighted, (B) arterial phase, (C) portal phase, (D) transitional phase, (E) hepatobiliary phase, (F) T2-weighted, and (G) diffusion-weighted (b = 800 s/mm^2) images, as well as (H) apparent diffusion coefficient map, reveal a 4.5-cm well-defined mass in the right liver dome. The mass exhibits rim hyperenhancement in the arterial phase (B), a targetoid appearance in the transitional and hepatobiliary phases (D, E), hyperintensity on the T2-weighted image (F), and diffusion restriction (G, H). The lesion is situated peripherally in the liver without evidence of adjacent biliary dilatation. The patient underwent central lobectomy, and iCCA was confirmed. Next-generation sequencing identified an *IDH1* missense mutation.